Suplemento de la Revista Mexicana de Física **3** 0308094 (2022) 1–5

Proton image and momentum distributions on the light-front

E. Ydrefors

Instituto Tecnológico de Aeronáutica, DCTA, 12228-900 São José dos Campos, Brazil.
Institute of Modern Physics, Chinese Academy of Sciences, Lanzhou 73000, China

T. Frederico

Instituto Tecnológico de Aeronáutica, DCTA, 12228-900 São José dos Campos, Brazil

Received 12 January 2022; accepted 20 April 2022

The proton has been studied in a fully dynamical three-body model on the light-front. The model is based on the concept of a strongly interacting diquark, either bound or virtual, which is generated from a zero-range interaction between the two active quarks. The obtained results for the Dirac electromagnetic form factor and also the density in the Ioffe-time space are shown and discussed. Additionally, we present results for the parton distribution function of the proton.

Keywords: Light-front dynamics; relativistic three-body systems; proton structure.

DOI: https://doi.org/10.31349/SuplRevMexFis.3.0308094

1. Introduction

The wave function of the proton on the null-plane, $x^+ = t + z = 0$, can in the Fock space be expressed in terms of its fundamental degrees of freedom (*i.e.* strongly interacting quarks and gluons), where each contribution is associated with a well-defined probabilility. From the light-front (LF) wave function (see *e.g.* [1]) many important physical quantities can be obtained, *e.g.* the electromagnetic form factors, the parton distribution function (PDF), the generalized parton distributions (GPDs) and the transverse momentum distribution (TMDs). Furthermore, the wave function in the configuration space associated with the null-plane, spanned by the transverse momentum coordinates and the Ioffe times, is obtained through a Fourier transform of the corresponding one in momentum space (see *e.g.* [2]).

However, it is worthy to point out that the light-front hyperplane and the observables associated with it are solely defined in Minkowski space. Consequently, they cannot be directly obtained from calculations which resides in Euclidean space, such as Lattice QCD. For this reason studies of the proton performed directly in Minkowski space are important. One example of such an approach is the Basis Light-Front Quantization [3] which recently was adopted to study the proton [4].

In this work the proton is studied within a three-body model on the null-plane, by introducing a strongly interacting diquark (either bound or virtual one) where the two active quarks are interacting through contact interaction. The three-body LF and Bethe-Salpeter (BS) equations for the zero-range interaction were introduced already in 1992 by Frederico [5]. The valence LF equation was then further studied by Carbonell and Karmanov in Ref. [6]. More recently, the three-body BS equation including the infinite number of Fock components in the BS amplitude was solved by Ydrefors *et al.* in Euclidean space [7] and in Minkowski space [8, 9].

In this contribution we will present some results for the Dirac electromagnetic form factor and the PDF, and also for the Ioffe-time distribution. A more comprehensive treatment of the adopted formalism and also much more results from this study can be found in Ref. [10].

2. Brief summary of the three-body model

The model of the proton adopted in this work is based on the three-boson model introduced by Frederico in the seminal work [5], and is based on the zero-range interaction between the quarks. The valence LF wave function then reads [9]

$$\Psi_3(x_1,\vec{k}_{1\perp},x_2,\vec{k}_{2\perp},x_3,\vec{k}_{3\perp}) = \frac{\Gamma(x_1,\vec{k}_{1\perp})+\Gamma(x_2,\vec{k}_{2\perp})+\Gamma(x_3,\vec{k}_{3\perp})}{\sqrt{x_1x_2x_3}M_0^2(x_1,\vec{k}_{1\perp},x_2,\vec{k}_{2\perp},x_3,\vec{k}_{3\perp})}, \quad (1)$$

where

$$M_0^2(x_1,\vec{k}_{1\perp},x_2,\vec{k}_{2\perp},x_3,\vec{k}_{3\perp}) = \frac{\vec{k}_{1\perp}^2+m^2}{x_1} + \frac{\vec{k}_{2\perp}^2+m^2}{x_2} + \frac{\vec{k}_3^2+m^2}{x_3}. \quad (2)$$

Furthermore, $\Gamma(x_i,k_{i\perp})$ (with $i=1,2,3$) denotes the Faddeev component of the vertex function of the three-body bound state which obeys the integral equation [5, 10]

$$\Gamma(x,k_\perp) = \frac{\mathcal{F}(M_{12}^2)}{(2\pi)^3}\int_0^{1-x}\frac{dx'}{x'(1-x-x')} \times \int_0^\infty d^2k'_\perp \frac{\Gamma(x',k'_\perp)}{\widehat{M_0^2}-M_N^2}, \quad (3)$$

with

$$\widehat{M_0^2} = M_0^2(x,\vec{k}_\perp,x',\vec{k}'_\perp,1-x-x',-(\vec{k}_\perp+\vec{k}'_\perp)). \quad (4)$$

TABLE I. Constituent mass, scattering length, di-quark mass and three-body mass for the two considered models in this work. Additionally, it is shown the computed radius defined as $r_1 = \hbar c\sqrt{-6[dF_1/dQ^2]|_{Q^2=0}}$ where F_1 denotes the valence Dirac form factor.

Model	m [MeV]	$a\,[m^{-1}]$	M_2 [MeV]	$M_N\,[m]$	r_{F_1} [fm]
I	317	-1.84	...	2.97	0.97
II	362	3.60	681	2.60	0.72

and the two-quark scattering amplitude reads

$$\mathcal{F}(M_{12}^2) = \frac{\Theta(-M_{12}^2)}{\frac{1}{16\pi^2 y}\log\frac{1+y}{1-y} - \frac{1}{16\pi m a}} + \frac{\Theta(M_{12}^2)\Theta(4m^2 - M_{12}^2)}{\frac{1}{8\pi^2 y'}\arctan y' - \frac{1}{16\pi m a}}. \quad (5)$$

Here, a denotes the scattering length and the effective two-quark off-shell mass squared

$$M_{12}^2 = (1-x)M_N^2 - \frac{k_\perp^2 + (1-x)m^2}{x}. \quad (6)$$

As it was shown in Appendix A of Ref. [10], Eq. (3) can be derived by projecting the three-boson Bethe-Salpeter equation (see *e.g.* Ref. [9]) onto the light-front by using the quasipotential technique (see *e.g.* [11, 12]).

In the present work, Eq. (3) was solved by adopting a bi-cubic spline decompostion, for more details see [9]. We studied the proton within two possibilities for diquarks, namely an unbound case with $a < 0$ and a bound one with $a > 0$, corresponding to the two parameter sets in Table I. In these calculations the scattering length a was fitted to reproduce the global behaviour of the Dirac form factor at $Q^2 \leqslant 1$ GeV^2, which will be discussed in the next section.

3. Valence Dirac form factor and parton distribution function

The valence contribution to the Dirac form factor of the proton takes the form

$$F_1(Q^2) = \left\{\prod_{i=1}^{3}\int\frac{d^2k_{i\perp}}{(2\pi)^2}\int_0^1 dx_i\right\}\delta\left(1-\sum_{i=1}^{3}x_i\right) \times \delta\left(\sum_{i=1}^{3}\vec{k}_{i\perp}^{\,f}\right)\Psi_3^\dagger(x_1,\vec{k}_{1\perp}^{\,f},...)\Psi_3(x_1,\vec{k}_{1\perp}^{\,i},...), \quad (7)$$

where $Q^2 = \vec{q}_\perp\cdot\vec{q}_\perp$ and the magnitudes of the momenta of the final (f) and initial (i) states are given by

$$|\vec{k}_{i\perp}^{\,f(i)}|^2 = \left|\vec{k}_{i\perp} \pm \frac{\vec{q}_\perp}{2}x_i\right|^2, \quad i = 1,2$$

$$|\vec{k}_{3\perp}^{\,f(i)}|^2 = \left|\pm\frac{\vec{q}_\perp}{2}(x_3-1) - \vec{k}_{1\perp} - \vec{k}_{2\perp}\right|^2. \quad (8)$$

Here $-$ is to be used for f and $+$ for i.

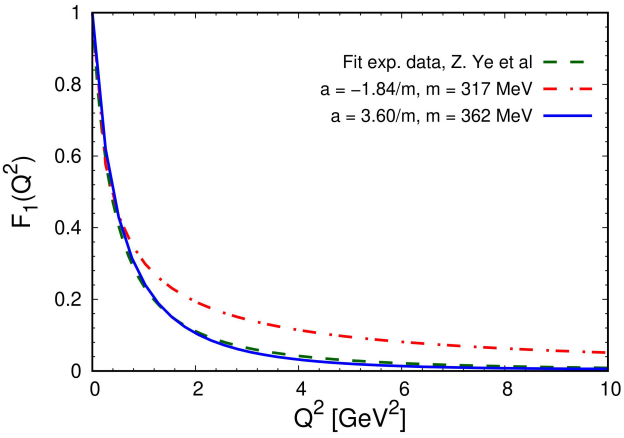

FIGURE 1. The calculated Dirac form factor (solid and dashed lines) compared with the empirical fit (dot-dashed line) of Ref. [13].

The calculated Dirac form factor for the two parameters sets of Table I is compared with the experimental fit of [13] in Fig. 1. It is seen that both parameter sets give a reasonable reproduction of the experimental data at $Q^2 < 1$ GeV^2. However, the model II with a bound diquark give a better agreement for larger values of the momentum transfer. The calculated value of the radius of 0.72 fm (see Table I) is also in fair agreement with the experimental one of 0.757 fm [14].

The single parton distribution function (PDF) is given by

$$f_1(x_1) = \frac{1}{(2\pi)^6}\int_0^{1-x_1}dx_2\int_0^1 dx_3\delta(1-x_1-x_2-x_3) \times \int d^2k_{1\perp}d^2k_{2\perp}d^2k_{3\perp}\delta(\vec{k}_{1\perp}+\vec{k}_{2\perp}+\vec{k}_{3\perp}) \times |\Psi_3(x_1,\vec{k}_{1\perp},x_2,\vec{k}_{2\perp},x_3,\vec{k}_{3\perp})|^2 = I_{11}+I_{22}+I_{33}+I_{12}+I_{13}+I_{23}, \quad (9)$$

and obeys the relation

$$\int_0^1 f_1(x_1)dx_1 = F_1(0) = 1. \quad (10)$$

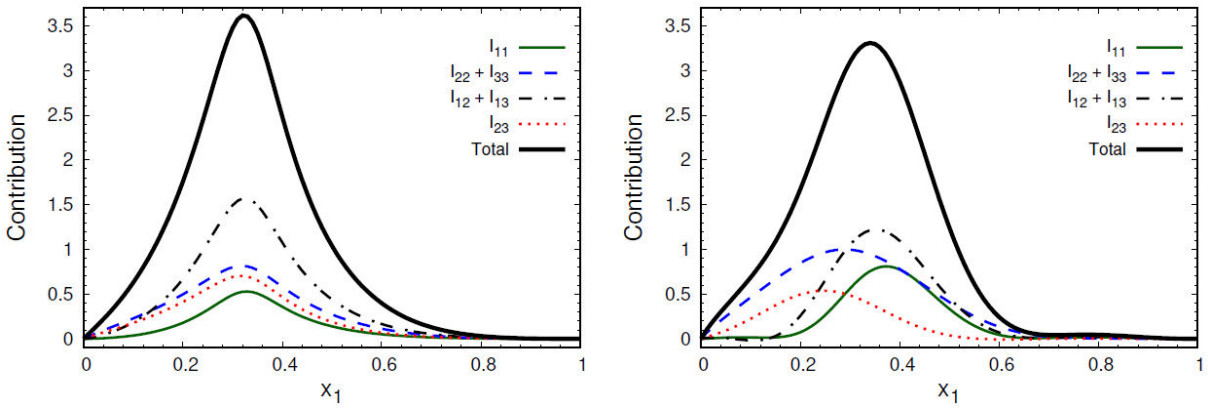

FIGURE 2. The contributions to the PDF for Model I (left panel) and Model II (right panel).

In Eq. (9) the Faddeev contributions take the forms

$$I_{ii} = \frac{1}{(2\pi)^6} \int_0^{1-x_1} dx_2 \int_0^1 \frac{dx_3}{x_1 x_2 x_3} \delta(1-x_1-x_2-x_3) \times \int d^2k_{1\perp} d^2k_{2\perp} d^2k_{3\perp} \delta(\vec{k}_{1\perp}+\vec{k}_{2\perp}+\vec{k}_{3\perp}) \times \frac{[\Gamma(x_i,\vec{k}_{i\perp})]^2}{(M_N^2 - M_0^2(x_1,\vec{k}_{1\perp},x_2,\vec{k}_{2\perp},x_3,\vec{k}_{3\perp}))^2}, \quad (11)$$

and for $i \neq j$

$$I_{ij} = \frac{2}{(2\pi)^6} \int_0^{1-x_1} dx_2 \int_0^1 \frac{dx_3}{x_1 x_2 x_3} \delta(1-x_1-x_2-x_3) \times \int d^2k_{1\perp} d^2k_{2\perp} d^2k_{3\perp} \delta(\vec{k}_{1\perp}+\vec{k}_{2\perp}+\vec{k}_{3\perp}) \times \frac{\Gamma(x_i,\vec{k}_{i\perp})\Gamma(x_j,\vec{k}_{j\perp})}{(M_N^2 - M_0^2(x_1,\vec{k}_{1\perp},x_2,\vec{k}_{2\perp},x_3,\vec{k}_{3\perp}))^2}. \quad (12)$$

Moreover, due to the symmetry of the wave function with respect to the exchange of particles 2 and 3, one has the equalities

$$I_{22} = I_{33}, \quad I_{12} = I_{13}. \quad (13)$$

In the two panels of Fig. 2, the computed contributions to the PDF are shown for models I and II, respectively. In each panel the total PDF is also displayed with a thick line. As it is seen in the left panel, for $a = -1.84/m$, the different contributions have similar shapes. On the contrary, for the bound diquark case in the right panel, they show quite different behaviours. Also, a significant damping is seen for $x_1 \geqslant 0.7$. As was pointed out in Ref. [10], this is related to the fact that for $a > 0$ the lowest energy solution is unphysical, *i.e.* having $M_N^2 < 0$. The lowest physical state is then an excited state and the vertex function $\Gamma(x, k_\perp)$ has nodes. The unphysical ground state can be removed by introducing a momentum cut-off $\mu \sim 1$ GeV. Calculations with such a cut-off are already under development and will be published elsewhere.

4. Ioffe-time image of the proton

The proton wave function can also be written in the configuration space related to the null plane ($x^+ = 0$), in terms of the transverse variables $b_{i\perp}$ and the Ioffe-times $\tilde{x}_i = b_i^- p^+$. The valence LF wave function in this representation is obtained as a Fourier transform of the momentum-space one, *i.e.*

$$\tilde{\Psi}_3(\tilde{x}_1,\vec{b}_{1\perp},...) = \left\{ \prod_{i=1}^3 \int \frac{d^2k_{i\perp}}{(2\pi)^2} \int_0^1 \frac{dx_i}{2\pi} e^{i\tilde{x}_i x_i - i\vec{b}_{i\perp}\cdot\vec{k}_{i\perp}} \right\} \times \delta\left(1-\sum_{i=1}^3 x_i\right) \delta\left(\sum_{i=1}^3 \vec{k}_{i\perp}\right) \Psi_3(x_1,\vec{k}_{1\perp},...). \quad (14)$$

The image of the proton is then provided by the probability density $|(\Psi_3(\tilde{x}_1,\vec{b}_{1\perp},...)|^2$. In Ref. [15] such a study was done for the pion.

In this work we consider for simplicity the special case:

$$\Phi(\tilde{x}_1,\tilde{x}_2) = \tilde{\Psi}_3(\tilde{x}_1,\vec{0}_\perp,\tilde{x_2},\vec{0}_\perp) = \int_0^1 dx_1 e^{i\tilde{x_1}x_1} \int_0^{1-x_1} dx_2 \int_0^1 dx_3 \times \delta(1-x_1-x_2-x_3) e^{i\tilde{x}_2 x_2} \phi(x_1,x_2,x_3), \quad (15)$$

with the distribution amplitude

$$\phi(x_1,x_2,x_3) = \int d^2k_{1\perp} d^2k_{2\perp} d^2k_{3\perp} \delta(\vec{k}_{1\perp}+\vec{k}_{2\perp}+\vec{k}_{3\perp}) \times \Psi_3(x_1,\vec{k}_{1\perp},x_2,\vec{k}_{2\perp},x_3,\vec{k}_{3\perp}). \quad (16)$$

In Fig. 3, we show the square of the magnitude of the wave function with respect to $\tilde{x}_1$ for two values of x_2, namely $\tilde{x}_2 = 0$ and $\tilde{x}_2 = 10$, for the two considered parameter sets.

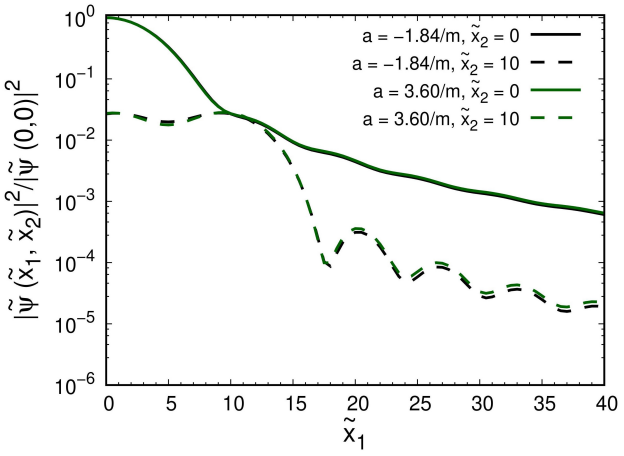

FIGURE 3. The modulus squared of the Ioffe-time distribution versus $\tilde{x}_1$ for two fixed values of $\tilde{x}_2$, *i.e.* $\tilde{x}_2 = 0$ and $\tilde{x}_2 = 10$. Results are displayed for Model I (blue lines) and Model II (red lines).

The results for Model I and II are almost the same. Additionally, for $\tilde{x}_2 = 10$ and $\tilde{x}_1 \geqslant 10$, a dramatic decrease of the amplitude is seen. An oscillatory pattern at larger values of $\tilde{x}_1$ can also be noticed. We see an exponential damping of the probability density versus the relative difference between the Ioffe time of the two quarks. One would expect this effect to be even more significant if confinement is included, since it is more effective at larger distances.

5. Conclusion

In this work we have studied the proton on the null plane ($x^+ = 0$) in a fully dynamical three-body model in the valence approximation, based on a contact interaction between the quarks. The diquark picture has been implemented through the assumption of a pole in the two-quark scattering amplitude, corresponding to either a virtual or bound two-body state. We have computed the Dirac electromagnetic form factor and also the parton distribution function. We also performed the Fourier transform to obtain the wave function in terms of the Ioffe-time variables, which together with the transverse variables provide the image of the proton.

In the near future, we plan to improve our model by introducing a momentum cut-off to remove the unphysical ground state which occur in the model for the bound diquark case. We will also attempt to introduce the spin degree-of-freedom in the model.

Acknowledgements

The work is a part of the project INCT-FNA proc. No. 464898/2014-5. The study has been supported partly by Conselho Nacional de Desenvolvimento Científico e Tecnológico (CNPq) under the grant 308486/2015-3 (TF). E.Y. is thankful for the financial support from the grants #2016/25143-7 and #2018/21758-2 from FAPESP. We also acknowledge the FAPESP Thematic Projects grants #13/26258-4 and #17/05660-0.

1. S. J. Brodsky, H.-C. Pauli, and S. S. Pinsky, *Quantum chromodynamics and other field theories on the light cone*, Phys. Rep., **301** (1998) 299. https://doi.org/10.1016/S0370-1573(97)00089-6.

2. G. A. Miller and S. J. Brodsky, *The frame-independent spatial coordinate $\tilde{z}$: Implications for light-front wave functions, deep inelastic scattering, light-front holography, and lattice QCD calculations*, Phys. Rev. C, **102** (2020) 022201. https://doi.org/10.1103/PhysRevC.102.022201.

3. J. Vary, H. Honkanen, J. Li, P. Maris, S. Brodsky, A. Harindranath, G. de Teramond, P. Sternberg, E. Ng, and C. Yang, *Hamiltonian light-front field theory in a basis function approach*, Phys. Rev. C, **81**(2010) 035205. https://doi.org/10.1103/PhysRevC.81.035205.

4. C. Mondal, S. Xu, J. Lan, X. Zhao, Y. Li, D. Chakrabarti, and J. P. Vary (BLFQ Collaboration), *Proton structure from a light-front Hamiltonian*, Phys. Rev. D, **102** (2020) 016008. https://doi.org/10.1103/PhysRevD.102.016008.

5. T. Frederico, *Null-plane model of three bosons with zero-range interaction*, Phys. Lett. B, **282** (1992) 409. https://doi.org/10.1016/0370-2693(92)90661-M.

6. J. Carbonell, and V. A. Karmanov, *Three-boson relativistic bound states with zero-range two-body interaction*, Phys. Rev. C, **67** (2003) 037001. https://doi.org/10.1103/PhysRevC.67.037001.

7. E. Ydrefors, J. H. Alvarenga Nogueira, V. Gigante, T. Frederico, and V. A. Karmanov, *Three-body bound states with zero-range interaction in the Bethe-Salpeter approach*, Phys. Lett. B, **770** (2017) 131. http://dx.doi.org/10.1016/j.physletb.2017.04.035.

8. E. Ydrefors, J. H. Alvarenga Nogueira, V. A. Karmanov, and T. Frederico, *Solving the three-body bound-state Bethe-Salpeter equation in Minkowski space*, Phys. Lett. B, **791** (2019) 276. https://doi.org/10.1016/j.physletb.2019.02.046.

9. E. Ydrefors, J. H. Alvarenga Nogueira, V. A. Karmanov, and T. Frederico, *Three-boson bound states in Minkowski space with contact interactions*, Phys. Rev. D, **101** (2020) 096018. https://doi.org/10.1103/PhysRevD.101.096018.

10. E. Ydrefors, and T. Frederico, *Proton image and momentum distributions from light-front dynamics*, Phys. Rev. D, **104** (2021) 114012. https://doi.org/10.1103/PhysRevD.104.114012.

11. T. Frederico, and G. Salmè, *Projecting the Bethe-Salpeter Equation onto the Light-Front and Back: A Short Review*,

Few-Body Syst., **49** (2011) 163. https://doi.org/10.1007/s00601-010-0163-z.

12. J. A. O. Marinho, and T. Frederico, *Next-to-leading order light-front three-body dynamics*, Proc. Sci., **LC2008** (2008) 036. https://doi.org/10.22323/1.061.0036.
13. Z. Ye, J. Arrington, R. J. Hill, and G. Lee, *Proton and neutron electromagnetic form factors and uncertainties*, Phys. Lett. B, **777**, (2018) 8. https://doi.org/10.1016/j.physletb.2017.11.023.
14. W. Xiong et al, *A small proton charge radius from an electron-proton scattering experiment*, Nature, **575** (2019) 147. https://doi.org/10.1038/s41586-019-1721-2.
15. W. de Paula, E. Ydrefors, J. H. Alvarenga Nogueira, T. Frederico, and G. Salmè, *Observing the Minkowskian dynamics of the pion on the null-plane*, Phys. Rev. D, **103**, (2021) 014002. https://doi.org/10.1103/PhysRevD.103.014002.